치의학박사 학위논문

Making three-dimensional Monson's sphere using virtual dental models

가상모형을 이용한 3 차원적 몬슨 구에 대한 연구

2013 년 8 월

서울대학교 대학원

치의학과 구강해부학 전공

남 신 은

치의학박사 학위논문

Making three-dimensional Monson's sphere using virtual dental models

가상모형을 이용한 3 차원적 몬슨 구에 대한 연구

2013 년 8 월

서울대학교 대학원

치의학과 구강해부학 전공

남 신 은

ABSTRACT

Making three-dimensional Monson's sphere using virtual dental models

Shin-Eun Nam

Department of Oral Anatomy

Graduate School

Seoul National University

(Directed by Professor, Seung-Pyo Lee, D.D.S., M.S.D., Ph.D.)

The Monson’s sphere and curve of Wilson can be used as reference for prosthetic reconstructions or orthodontic treatments. This study aimed to generate and measure the three-dimensional (3-D) Monson’s sphere and curve of Wilson using virtual dental models and custom software. Mandibular dental casts from 68 young adults of Korean descent were scanned and rendered as virtual dental models using a 3-D digitizing scanner. 26 landmarks were digitized on the virtual dental models using a custom made software program. The Monson’s sphere was estimated by fitting a sphere to the cusp tips using a least-squares method. Two curves of Wilson were generated by finding the intersecting circle between the Monson’s sphere and two vertical planes orthogonal to a virtual occlusal plane. Non-parametric Mann-Whitney and Kruskal-Wallis tests were performed to test for difference between sex and in cusp number within tooth position. The mean radius of Monson’s sphere was 110.89 ± 25.75 mm. There were significant differences between males and

females in all measurements taken ($p < 0.01$), within 16.87 - 17.27 mm. Furthermore, morphological variation derived from variability in cusp number in the second premolar and second molar were not found to influence occlusal curvature ($p > 0.05$). This study describes a best-fit algorithm for generating 3-D Monson's sphere using occlusal curves quantified from virtual dental models. The radius of Monson's sphere in Korean subjects was greater than the original four-inch value suggested by Monson. The Monson's sphere and curve of Wilson can be used as a reference for prosthetic reconstruction and orthodontic treatment. The data found in this study may be applied to improve dental treatment results.

Keywords: Monson's sphere, curve of Wilson, virtual models, algorithm

Student number: 2007-23381

Making three-dimensional Monson's sphere using virtual dental models

Department of Oral Anatomy, School of Dentistry,

The Graduate School, Seoul National University

(Directed by Professor Seung-Pyo Lee)

Shin-Eun Nam

Contents

Ⅰ. Introduction

Two occlusal curvatures and an associated fitted sphere have been proposed to exist in the human occlusal dental arcade. The curve of Spee is an anterioposterior curve that passes through the cusp tips of the mandibular canines and the buccal cusp tips of the premolars and molars.[1] The curve of Wilson is a mediolateral curve that contacts the buccal and lingual cusp tips of both sides of the dental arch.[2] Monson described a three-dimensional (3-D) sphere combining the anterioposterior curve and the mediolateral curve, with the mandibular incisal edges and cusp tips touching the sphere.[3]

Occlusal curvatures are clinically important in dental treatment procedures.[4-8] The curve of Spee permits total posterior disclusion on the mandibular protrusion given proper anterior tooth guidance[1] and the curve of Wilson permits lateral mandibular excursion free from posterior interferences.[2] Monson's sphere has been used as a reference for prosthodontic reconstruction of the posterior dentition.[8]

It is essential to recognize the standard values of occlusal curvature for the diagnosis and rehabilitation of occlusal disharmony.[9] For the quantification of these occlusal curvatures, various methods have been developed. Conventional methods rely on measuring the depths or angles of the curvatures directly on dental casts using rulers,[10] analog calipers,[11,12] digital calipers,[4,13,14] and Broadrick occlusal plane analyzers.[8] Unfortunately, conventional direct measurements from dental casts are limited by not only the accessibility and repeatability in the cognition of reference points but are also restricted to intra-arch measurements.[15] Indirect measurements from 2-D scan images were used to overcome these problems and enabled a variety of analyses using the mathematical calculations or the aid of specialized software.[5,16,17] However, a true curve of Spee and curve of Wilson are not parallel to the sagittal plane or frontal plane unlike the conceptual diagrams

which depicts two curves in the frame of 2-D images.[1,2] Such measurements on 2-D images[5,16,17] were inevitable to address different values from true ones obtained by 3-D environment. Finally, it is impossible to generate Monson's sphere, which requires 3-D information including x-, y- and z-coordinate values,[3] using conventional methods. Therefore, it is necessary to use 3-D tools to comprehend true occlusal curvatures.

Occlusal curvature studies using 3-D tools have usually employed 3-D digitizers.[6,15,18] Ferrario et al.[6] were the first to obtain x-, y- and z-coordinates of cusp tips using a 3-D digitizer and derived a spherical model of the curvature of the occlusal surface. Using a 3-D digitizer, occlusal curvatures can be investigated by geometric-mathematical analyses based on reference points with 3-D coordinates.

Due to recent advances in engineering science and technology, dental research using three-dimensionally reconstructed virtual dental models has been introduced and is widely applied nowadays.[19-27] With the addition of specialized software, several studies have demonstrated that the virtual dental models allow increased recognition accuracy and enable complicated geometric calculations.[22,26]

Until now, most occlusal curvature studies have focused on the curve of Spee,[5,7,16,17,28,29] while the curve of Wilson and Monson's sphere have received little attention.[6,9,18] Although, curve of Spee has been measured using virtual dental models,[7,30] meanwhile the generation of a real sphere, not a circle, is hard to achieve owing to the methodological limitation.

Therefore, the aim of this study was to generate the 3-D occlusal curvatures including Monson's sphere and curve of Wilson using virtual dental models and custom designed software. Also, the values of 3-D occlusal curvatures was measured and analyzed.

Ⅱ. Review of literature

1. Occlusal curvatures in human dentition

Bonwill[31] proposed the first scientific description in the development of occlusal theory in 1887. He suggested the equilateral triangle of four-inches from condyle to condyle and from condyle to mesioincisal angle of the mandibular central incisors and an arrangement of artificial teeth in the plane of that.[31]

Spee[1] described the anterioposterior occlusal curve, not a plane, in sagittal view in 1890. He defined the curve of occlusion as the line on a cylinder that is tangent to the anterior border of the condyle, the occlusal surface of the second molar, and the incisal edges of the mandibular incisors, this curvature was termed the curve of Spee.[1] He suggested that this geometric arrangement defined the most efficient pattern for maintaining maximum tooth contacts during chewing and considered it an important tenet in denture construction.[1,4] Wilson[2] suggested a mediolateral occlusal curve that contacts the buccal and lingual cusp tips of both sides of the dental arch in frontal view in 1911.

Bonwill's idea was advanced by Monson in 1920.[3] Monson[3] described a 3-D sphere combining the anterioposterior curve and mediolateral curve, with the mandibular incisal edges and cusp tips touching the four-inch sphere. It is referred to as Monson's spherical theory.

2. Measurements of occlusal curvature

Many studies have suggested the occlusal curvature with various measurement methods. Conventionally, occlusal curvatures were measured manually on mandibular stone model[29,32,33] with rulers[10], analogue calipers[11,12], digital calipers[4,13,14] and specialized tools such as Broadrick occlusal plane analyzers.[8]

Unfortunately, conventional direct measurements from dental casts are limited by not only the accessibility and repeatability in the cognition of reference points but are also restricted to intra-arch measurements.[15]

Indirect measurements from 2-D scan images were used to overcome these problems and enabled a variety of analyses using the mathematical calculations or the aid of specialized software.[5,8,16,17,28,34,35,36] When the arrangement of mandibular dentition considered,[10] a true curve of Spee and curve of Wilson are not parallel to the sagittal plane or frontal plane unlike the conceptual diagrams which depicts two curves in the frame of 2-D images.[1,2] Such measurements, had usually been made on separate 2-D planes, were inevitable to address different values from true ones obtained by 3-D environment, thus losing some of the original 3-D information.[6] Moreover, it is impossible to generate Monson's sphere, which requires 3-D information including x, y, z coordinate values,[3] using conventional methods. Therefore, it is necessary to use 3-D tools to comprehend true occlusal curvatures.

Occlusal curvature studies using 3-D tools have usually employed 3-D digitizers.[6,15,18] Using a 3-D digitizer, occlusal curvatures can be investigated by geometric-mathematical analyses based on reference points with 3-D coordinates. Ferrario et al.[6] were the first to report the quantitative data to support Monson's classical four inch sphere. They obtained x, y, z coordinates of cusp tips using a 3-D digitizer and derived a spherical model of the curvature of the occlusal surface. From the best interpolate sphere the radius of the right and left curves of Spee and of the canine and molar curves of Wilson were computed. Hayasaki et al.[15] introduced a new software for cast analysis by using a mechanical 3-D digitizing system and evaluated bias in relation to the measurements obtained with digital calipers in occlusal curvature measurements. Occlusal curvature studies, had focused on the curve of Spee,[5,7,16,17,28,29] have been expanded the range even further by an adoption of 3-D tools.[6,9,18] However, the generation of a real sphere, not a

circle, is hard to achieve owing to the methodological limitation.

3. Virtual models in dentistry

Recent advances in technology have generated a variety of techniques for medical imaging.[37] One of these initially developed for industry is laser surface scanning, which is a noninvasive method for acquiring 3-D images.[30] In dentistry, three-dimensionally reconstructed virtual models are available for various dental researches, supplemented by dedicated software to perform the necessary measurements.[37-44] Several studies have demonstrated that the virtual dental models allow increased recognition accuracy and enable complicated geometric calculation.[22,26,45]

4. Virtual dental models in occlusal curvature measurements

There has been minimal research regarding the occlusal curvature using virtual dental models. Cheon et al.[7] first investigated the curve of Spee with a virtual dental models and evaluated the relationship between the curve of Spee and dentofacial measurements from 2-D cephalograms. In the study, the curve of Spee was measured the perpendicular distances from the virtual occlusal plane to the buccal cusp tip of each lateral tooth, and the deepest point was used as a representative values the curve of Spee.

It has been reported recently a comparison of conventional method using mandibular dental casts with ruler and virtual measurement method using 3-D model analogues in curve of Spee measurements.[30] The authors evaluated the potential of 3-D models for measurement of curve of Spee and concluded that it is useful tool for analysis of depth of curve of Spee and treatment planning.[30]

Those measurements are significant in the sense that it used the virtual dental models shown to be accurate and reproducible.[7] There is, to my knowledge, no

study in curve of Wilson and Monson's sphere using virtual dental models and no generation of a real Monson's sphere.

Ⅲ. Materials and Methods

1. Subjects

Mandibular dental casts of 41 Korean males and 27 Korean females were prepared (Table 1). Subjects were selected based on the following criteria: (1) complete permanent dentition except for third molars; (2) absence of cuspal coverage restorations in the canines and posterior teeth ; (3) no previous or current orthodontic treatment; and (4) less than 3 mm of crowding and/or spacing for the entire mandibular dental arch. This study was approved by the Institutional Review Board (IRB) of the College of Dentistry, Seoul National University (IRB No. S-D20100011).

2. Reconstruction of virtual dental models

3-D reconstructions of virtual dental models were performed according to a procedure previously described by Lee at al.[21] In brief, at first, dental casts were scanned using an optoTOP-HE 3-D system (Breuckmann GMBH, Meersburg, Germany), which has a point accuracy of 0.100 ± 0.005 mm and resolution of 0.015 to 0.500 mm in the X and Y axes and 0.002 mm in the Z axis.[46] Each cast was scanned using ten or more different views that were combined by a registration method (iterative closest point algorithm)[47-51] and merged and rendered as a virtual dental model using Rapidform XO software (INUS Technology, Seoul, South Korea).

3. Digitization of reference points

In this study, 26 reference points were generated to measure occlusal curvature beginning with the cusp tip of the canine and following the buccal and lingual cusp tips of the premolar and molar teeth on the right and left sides (Fig. 1). Normal variation in the number of lingual cusps in the second premolars and expression of the distal cusp in the second molars were noted in the study sample. The reference points were generated in all cusp tips of the teeth regardless of the cuspal variation. Additionally, all models were further classified into groups according to the cusp numbers of the second premolar and the second molar to determine differences in occlusal curvatures with the cuspal variation (Table 3). All the sample models in this study had the five-cusp first molars, which was not classified into groups. The third molars were excluded from the generation of reference points.

To reduce noise introduced by observer error, a custom made software program was applied. The program aided operators by providing a mechanism to specify the direction along which to measure the height of each vertex from a region of interest (Fig. 2A) and then automatically selecting the highest vertex and identifying it as the cusp tip (Fig. 2B). The height was measured parallel to the long axis of the tooth. The long axis was determined using the method described in literatures[42,52] and, although the process of specifying the direction of long axis was subjective, the remaining processes of reference point generation and measurement were not influenced by observer but performed reproducibly using the software. The reproducibility test is described in section 6. in detail.

The reference points used to estimate the occlusal curvature were cusp tips of the canine and the cusp tips of the posterior teeth. The positions of cusp tips are naturally shifted by occlusal tooth wear during aging.[43,53] However, the ages of the male and female samples used in this study were 23 to 26 years, minimizing the effects of tooth wear.

4. Monson's sphere fitting strategy

Monson's sphere was estimated by fitting a sphere to the cusp tip points from the first premolars to the second molars based on the least-squares algorithm (Appendix 1).[54] Fig. 3 shows various examples of fitted sphere generated by this method. The spheres were found under the condition of no constraints such as staying of the center of the sphere on a certain plane.

Prior to computing Wilson curves, it is necessary to generate the virtual occlusal plane (VOP) as a geometric reference plane. We used an orthogonal regression approach to define this plane, or a plane that was fitted to the cusp tip points from the canines to the second molars. Planar fitting was performed to minimize the squared sum of the orthogonal distances from sample points to a target plane (Appendix 2). Many researchers have used specific points to define this type of plane, such as the incisal edges of the central incisors,[29] the distobuccal cusps of the second molars[5,7] or the distal cusp tips of the most posterior teeth.[4,29] We chose the method described above because it represents the overall data points for representing the plane in a less biased manner (Fig. 4). That was, the occlusal plane was determined by a plane-fitting algorithm which incorporated the whole cusp tips as the target points. It used more points than the traditional ways of our knowledge do, it was rather unbiased.

5. Computation of Wilson curves

After the VOP was computed, two types of Wilson curves representing the anterior and posterior portions were defined. The first curve was computed by finding the intersection circle between Monson's sphere and a plane that passes through the right and left canine cusp tips and is orthogonal to the VOP. The second curve was found in a similar fashion but used the centroids of the four cusp tips of each first molar as the pass-through points (Figs. 5 and 6).

On average it took about 0.5 second to fit a sphere and compute curves against the reference points. The computing environment was quite a modern average personal computing one. A window XP PC with Pentium-5 CPU and 4 Gigabytes of main memory was used.

6. Reproducibility of measurement

All dental reference point generation and parameter measurements were performed by the same investigator. The only subjective process of this study is specifying the direction of the long axis. To test the reproducibility, 15 casts were selected at random and the digitization of landmarks was repeated after 3 months. The x-, y- and z-coordinate values of each reference point were given and the error was measured for all selected models using the intraclass correlation coefficient (ICC), revealing excellent coefficient values (ICC = 0.953 – 0.999, $p < 0.001$).

7. Statistical analysis

Statistical analysis was performed using SPSS 11.5 software for Windows (SPSS Inc., Chicago, IL, USA). The radii of Monson's spheres and curves of Wilson were examined using conventional descriptive statistics, and Mann-Whitney U tests were applied to determine differences in occlusal curvatures between males and females. Kruskal-Wallis tests were performed to determine whether there were significant differences related to morphological variation, or the presence of additional cusp tips. For all analyses, the significance level was set at 5% ($p < 0.05$).

Ⅳ. Results

The total mean radius of Monson's sphere was 110.89 ± 25.75 mm (5%

percentile, 72.04 mm; 95% percentile, 164.63 mm) and was therefore larger than the original four-inch value described by Monson.[3] Descriptive statistics of other variables studied are presented in Table 2. There were significant differences between males and females in all measurements ($p < 0.01$). Inparticular, the greatest difference was found in the curve of Wilson among the canine teeth. Fig. 7 shows sex differences in Monson's sphere, curve of Wilson in canines and curve of Wilson in molars from male (Fig. 7A) and female (Fig. 7B) sample models.

The number of lingual cusps in the second premolars and the prevalence of the distal cusp in second molars did not significantly influence the radius of occlusal curvature, respectively ($p > 0.05$) (Table 3). Accordingly, these two dental morphological variations were not considered to affect measurements taken of the radius of occlusal curvature.

Ⅴ. Discussion

In the present study, a best-fit algorithm for producing the 3-D Monson's sphere was developed and measurements of the radius of the resultant occlusal curves were performed. Many studies have reported the curvature of the natural human dentition.[4,5,8,11,13,14,16,17,33,34,35,36] However, few studies have been undertaken to analyze the 3-D morphology of occlusal surfaces. Ferrario et al.[6,18] analyzed the 3-D intrinsic characteristics of occlusal curvature from a mathematical and statistical point of view using a 3-D digitizer. Recently, 3-D occlusal curvature in young Japanese adults was estimated by calculating the radius and center position of the approximate sphere using Ferrario's method[6] with minor modifications for the digitization of arches using the Broadrick occlusal analyzer.[9] Although an approximate sphere was generated using 3-D coordinate reference points, the radius and center of the sphere were determined with the x-axis set at zero and the

center on the *y*-*z* plane. The generation of 3-D intrinsic characteristics of occlusal curvatures was therefore limited in these previous studies. Therefore, this study used virtual dental models scanned and rendered using a 3-D scanner to overcome the limitation.

In this study, reference points were determined using a custom software program that automatically detected the highest cusp tip points with respect to operator-defined directions for each tooth. This software allowed operators to make more appropriate assessments, although observer error may have affected the process of specifying the direction of long axis or the generation of reference points. Therefore, we tried to find the reproducibility of them and the results were found to be highly reliable.

Identifying a best-fit sphere based on the sample points is an inherently non-linear problem. In this study we used a gradient descent method, also known as steepest descent, to find the solutions. Conceptually, the steepest descent method is an iterative method and a local minimum algorithm. Like all other local optimization problems, it is very sensitive to initial guesses and the quality of sample points used. In this study, centroids of the sample points were used as the initial guess points and the maximum number of iterations was set to 1,000,000. There were no cases of failure. The fitting method itself is similar to that used in Ferrario's study,[6] with the exception that the sphere centre was not confined to lie in an arbitrary plane. In the present study, full 3-D degrees of freedom were incorporated. Thus, this study represents 3-D Monson's sphere using an explicit model that had previously only been described in conceptual terms.[6,9,18]

Wilson's curve was defined as the intersection circle between Monson's sphere and a plane orthogonal to a virtual occlusal plane. Geometrically, a set of three points that are non-colinear is a necessary and sufficient condition for defining a

plane embedded in 3-D space. Many previous studies were based on this principle for defining an occlusal plane with two posterior cusp tips and derived incisor edge.[4,5,7,29] However, we aimed to better reflect true occlusal curvature. A least squares-based approach for finding the plane minimizing the sums of orthogonal distances from individual sample points to the plane is well-supported.[54] The plane passes through the centroid of the sample points and has a normal vector that is the eigenvector with the smallest eigenvalue of the sample point covariance matrix. In other words, the geometric fitting of the plane/sphere, which considers all of the reference points, was performed to estimate occlusal curvature based on the least squares method in virtual dental models. Two types of distance measures are normally used to define the cost or objective function of a plane fitting algorithm. One is algebraic and the other is geometric. As stated above, what we employed was the orthogonal Euclidean distance from a datum to a plane, which allowed a geometric approach. This complicated approach for defining an occlusal plane buffers and averages the noises inherent in all dental data by incorporating more samples into the calculation.

The total mean radius of Monson's sphere was 110.89 ± 25.75 mm, which was larger than the original four-inch value suggested by Monson[3] or European young adults data (101.30 ± 23.56 mm).[18] However, another study using 3-D models of Asian young adults showed similar results with this study 110.6 mm.[9] These differences could result from both population-based and methodological differences. At this time, it is ambiguous which factor has more influence on these differences, and further investigation is needed.

The measured mean radius of Monson's sphere was influenced by sex, with a mean difference of 16.87 mm ($p < 0.01$). Regarding occlusal curves most studies have focused to curve of Spee, and suggested no significant sex differences,[5-

[7,16,17,32] although there is no consensus for Monson's sphere.[6,9] However, there is significant sex difference in arch width[32,55] which is related with Monson's sphere, and supports the sex difference in Monson's sphere radius.

The number of cusps in the mandibular posterior teeth is variable. For instance, among the mandibular second premolar the three-cusp variant is found more frequently than the two-cusp variant in some populations.[56] In some cases, the mandibular first molars lack the distal cusp.[57] The five-cusp type mandibular second molar is not uncommon with population-based characteristics.[57] In the sample utilized in the present study, the effect of cusp number on occlusal curvature was not found to be significant in the second premolar and second molar tooth positions ($p > 0.05$). On account of this, we did not consider morphological differences of the posterior teeth during the clinical rehabilitation of occlusal curvature.

Monson's sphere has been used as a reference for the ideal occlusal model in prosthodontic restoration of the natural dentition[8] and for considerations of cusp inclination or height in arrangements of mandibular posterior artificial teeth.[31] Appropriate management is critical for the construction of stable complete dentures.[31] The curve of Wilson can be used to evaluate the arch extensions or buccal inclinations of the posterior dentition in orthodontic treatments. In this study, we described true occlusal curvature using a virtual dental model. Recently, dental CAD/CAM (computer-aided design and computer-aided manufacture) technology has developed and the use of virtual dental models became common in dentistry. Therefore, it seems that the data of the Monson's sphere and the Wilson's curve found in this study may be applied to improve treatment results.

Ⅵ. Conclusions

1. 3-D occlusal curvatures including the curve of Wilson and Monson’s sphere were generated in the 3-D coordinate system using virtual dental models.

2. The radius of Monson’s sphere in Korean subjects was greater than the original four-inch value suggested by Monson. The difference was particularly noticeable in males ($p < 0.01$).

3. The data of the Monson's sphere and the Wilson's curve found in this study may be applied to improve treatment results, especially for the dental prosthetic and orthodontic treatments.

References

1. Spee FG. Die Verschiebungsbahn des Unterkiefers am Schädel. *Archives fur Anatomie und Physiologie* 1890;16:285-294.

2. Wilson GH. A manual of dental prosthetics. Philadelphia: Lea & Febiger; 1911. p.22-37.

3. Monson GS. Occlusion as applied to crown and bridgework. *The Journal of the National Dental Association* 1920;7:399-413.

4. Marshall SD, Caspersen M, Hardinger RR, Franciscus RG, Aquilino SA, Southard TE. Development of the curve of Spee. *American Journal of Orthodontics and Dentofacial Orthopedics* 2008;134:344-352.

5. Xu H, Suzuki T, Muronoi M, Ooya K. An evaluation of the curve of Spee in the maxilla and mandible of human permanent healthy dentitions. *The Journal of Prosthetic Dentistry* 2004;92:536-539.

6. Ferrario VF, Sforza C, Miani Jr. A. Statistical evaluation of Monson's sphere in healthy permanent dentitions in man. *Archives of Oral Biology* 1997;42:365-369.

7. Cheon SH, Park YH, Paik KS, Ahn SJ, Hayashi K, Yi WJ, Lee SP. Relationship between the curve of Spee and dentofacial morphology evaluated with a 3-dimensional reconstruction method in Korean adults. *American Journal of Orthodontics and Dentofacial Orthopedics* 2008;133:640 e7-14.

8. Lynch CD, McConnell RJ. Prosthodontic management of the curve of Spee: use of the Broadrick flag. *The Journal of Prosthetic Dentistry* 2002;87:593-597.

9. Kagaya K, Minami I, Nakamura T, Sato M, Ueno T, Igarashi Y. Three-dimensional analysis of occlusal curvature in healthy Japanese young adults. *Journal of Oral Rehabilitation* 2009;36:257-263.

10. Andrews LF. The six keys to normal occlusion. *American Journal of Orthodontics* 1972;62:296-309.

11. Little RM. The irregularity index: a quantitative score of mandibular anterior alignment. *American Journal of Orthodontics* 1975;68:554-563.

12. Bolton WA. Disharmony in tooth size and its relation to the analysis and treatment of malocclusion. *Angle Orthod* 1958;28:113-130.

13. Harris EF. A longitudinal study of arch size and form in untreated adults. *American Journal of Orthodontics and Dentofacial Orthopedics* 1997;111:419-427.

14. Warren JJ, Bishara SE. Comparison of dental arch measurements in the primary dentition between contemporary and historic samples. *American Journal of Orthodontics and Dentofacial Orthopedics* 2001;119:211-215.

15. Hayasaki H, Martins RP, Gandini LG, Saitoh I, Nonaka K. A new way of analyzing occlusion 3 dimensionally. *American Journal of Orthodontics and Dentofacial Orthopedics* 2005;128:128-132.

16. Ferrario VF, Sforza C, Miani Jr. A, Colombo A, Tartaglia G. Mathematical definition of the curve of Spee in permanent healthy dentitions in man. *Archives of Oral Biology* 1992;37:691-694.

17. Craddock HL, Lynch CD, Franklin P, Youngson CC, Manogue M. A study of the proximity of the Broadrick ideal occlusal curve to the existing occlusal curve in dentate patients. *Journal of Oral Rehabilitation* 2005;32:895-900.

18. Ferrario VF, Sforza C, Poggio CE, Serrao G, Colombo A. Three-dimensional dental arch curvature in human adolescents and adults. *American Journal of Orthodontics and Dentofacial Orthopedics* 1999;115:401-405.

19. Krarup S, Darvann TA, Larsen P, Marsh JL, Kreiborg S. Three-dimensional analysis of mandibular growth and tooth eruption. *Journal of Anatomy* 2005;207:669-682.

20. Park YS, Lee SP, Paik KS. The three-dimensional relationship on a virtual model between the maxillary anterior teeth and incisive papilla. *The Journal of*

Prosthetic Dentistry 2007;98:312-318.

21. Lee SP, Delong R, Hodges JS, Hayashi K, Lee JB. Predicting first molar width using virtual models of dental arches. *Clinical Anatomy* 2008;21:27-32.

22. DeLong R, Heinzen M, Hodges JS, Ko CC, Douglas WH. Accuracy of a system for creating 3D computer models of dental arches. *Journal of Dental Research* 2003;82:438-442.

23. Tolleson SR, Kau CH, Lee RP, English JD, Harila V, Pirttiniemi P, Valkama M. 3-D analysis of facial asymmetry in children with hip dysplasia. *Angle Orthod* 2010;80:519-524.

24. Kwon JH, Son YH, Han CH, Kim S. Accuracy of implant impressions without impression copings: a three-dimensional analysis. *The Journal of Prosthetic Dentistry* 2011;105:367-373.

25. Kehl M, Swierkot K, Mengel R. Three-dimensional measurement of bone loss at implants in patients with periodontal disease. *Journal of Periodontology* 2011;82:689-699.

26. Redlich M, Weinstock T, Abed Y, Schneor R, Holdstein Y, Fischer A. A new system for scanning, measuring and analyzing dental casts based on a 3D holographic sensor. *Orthod Craniofac Res* 2008;11:90-95.

27. Nam SE, Kim YH, Park YS, Baek SH, Hayashi K, Kim KN, Lee SP. Three-dimensional dental model constructed from an average dental form. *American Journal of Orthodontics and Dentofacial Orthopedics* 2012;141:213-218.

28. Osborn JW. Orientation of the masseter muscle and the curve of Spee in relation to crushing forces on the molar teeth of primates. *American Journal of Physical Anthropology* 1993;92:99-106.

29. Baydas B, Yavuz I, Atasaral N, Ceylan I, Dagsuyu IM. Investigation of the changes in the positions of upper and lower incisors, overjet, overbite, and

irregularity index in subjects with different depths of curve of Spee. *Angle Orthod* 2004;74:349-355.

30. Adaskevicius R, Svalkauskiene V. Measurement of the Depth of Spee's Curve using Digital 3D Dental Models. *Electronics and Electrical Engineering* 2011;109:53-56.

31. Bonwill WGA. The geometrical and mechanical laws of the articulation of the human teeth: the anatomical articulator. In: Litch F, editor. The american system of dentistry. Philadelphia: Lea Brothers; 1887. p.486-498.

32. Merz ML, Isaacson RJ, Germane N, Rubenstein LK. Tooth diameters and arch perimeters in a black and a white population. *American Journal of Orthodontics and Dentofacial Orthopedics* 1991;100:53-58.

33. Shannon KR, Nanda RS. Changes in the curve of Spee with treatment and at 2 years posttreatment. *American Journal of Orthodontics and Dentofacial Orthopedics* 2004;125:589-596.

34. Osborn JW. Relationship between the mandibular condyle and the occlusal plane during hominid evolution: some of its effects on jaw mechanics. *American Journal of Physical Anthropology* 1987;73:193-207.

35. Osborn JW, Francis LJ. The position of the dentition in the mandible and its possible relation to orthodontic abnormalities. *American Journal of Orthodontics and Dentofacial Orthopedics* 1989;96:327-332.

36. De Praeter J, Dermaut L, Martens G, Kuijpers-Jagtman AM. Long-term stability of the leveling of the curve of Spee. *American Journal of Orthodontics and Dentofacial Orthopedics* 2002;121:266-272.

37. Da Silveira AC, Daw JL, Jr., Kusnoto B, Evans C, Cohen M. Craniofacial applications of three-dimensional laser surface scanning. *Journal of Craniofacial Surgery* 2003;14:449-456.

38. Kau CH, Richmond S, Incrapera A, English J, Xia JJ. Three-dimensional surface acquisition systems for the study of facial morphology and their application to maxillofacial surgery. *Int J Med Robot* 2007;3:97-110.

39. Chen H, Lowe AA, de Almeida FR, Wong M, Fleetham JA, Wang B. Three-dimensional computer-assisted study model analysis of long-term oral-appliance wear. Part 1: Methodology. *American Journal of Orthodontics and Dentofacial Orthopedics* 2008;134:393-407.

40. Rodriguez JM, Bartlett DW. The dimensional stability of impression materials and its effect on in vitro tooth wear studies. *Dental Materials* 2011;27:253-258.

41. Lee SP, Lee SJ, Hayashi K, Park YS. A three-dimensional analysis of the perceived proportions of maxillary anterior teeth. *Acta Odontologica Scandinavica* 2012;70:432-440.

42. Tanoi A, Motegi E, Sueishi K. Change in dentition over 20 years from third decade of life. *Orthodontic Waves* 2012;71:90-98.

43. Lee SP, Nam SE, Lee YM, Park YS, Hayashi K, Lee JB. The development of quantitative methods using virtual models for the measurement of tooth wear. *Clinical Anatomy* 2012;25:347-358.

44. Kau CH, Zhurov A, Richmond S, Bibb R, Sugar A, Knox J, Hartles F. The 3-dimensional construction of the average 11-year-old child face: a clinical evaluation and application. *Journal of Oral and Maxillofacial Surgery* 2006;64:1086-1092.

45. Nouri M, Massudi R, Bagheban AA, Azimi S, Fereidooni F. The accuracy of a 3-D laser scanner for crown width measurements. *Australian Orthodontic Journal* 2009;25:41-47.

46. Slizewski A, Semal P. Experiences with low and high cost 3D surface scanner. *Quartär* 2009;56:131-138.

47. Besl PJ, McKay ND. A method for registration of 3-D shapes. *IEEE Trans Patt Anal Machine Intell* 1992;14:239-256.

48. Perez SI, Bernal V, Gonzalez PN. Differences between sliding semi-landmark methods in geometric morphometrics, with an application to human craniofacial and dental variation. *Journal of Anatomy* 2006;208:769-784.

49. Swennen GRJ, Mommaerts MY, Abeloos J, De Clercq C, Lamoral P, Neyt N, Casselman J, Schutyser F. The use of a wax bite wafer and a double computed tomography scan procedure to obtain a three-dimensional augmented virtual skull model. *Journal of Craniofacial Surgery* 2007;18:533-539.

50. Swennen G, Mommaerts M, Abeloos J, De Clercq C, Lamoral P. A cone-beam CT based technique to augment the 3D virtual skull model with a detailed dental surface. *International Journal of Oral and Maxillofacial Surgery* 2009;38:48-57.

51. Lee CF, Li GJ, Wan SY, Lee WJ, Tzen KY, Chen CH, Song YL, Chou YF, Chen YS, Liu TC. Registration of micro-computed tomography and histological images of the guinea pig cochlea to construct an ear model using an iterative closest point algorithm. *Annals of Biomedical Engineering* 2010;38:1719-1727.

52. Fuma A, Motegi E, Fukagawa H, Nomura M, Kano M, Sueishi K, Okano S. Mesio-distal tooth angulation in elderly with many remaining teeth observed by 3-D imaging. *Bulletin of Tokyo Dental College* 2010;51:57-64.

53. Donachie MA, Walls AW. Assessment of tooth wear in an ageing population. *Journal of Dentistry* 1995;23:157-164.

54. Schomaker V WJ, Marsh RE, Bergman G. To fit a plane or a line to a set of points by least squares. *Acta Crystallographica* 1959;12:600-604.

55. Forster CM, Sunga E, Chung CH. Relationship between dental arch width and vertical facial morphology in untreated adults. *European Journal of Orthodontics* 2008;30:288-294.

56. Scheid RC. Woelfel's dental anatomy: its relevance to dentistry. 7th ed. Philadelphia: Lippincott Williams & Wilkins; 2007. p.209-228.

57. Kraus BS, Jordan RE, Abrams L. A study of masticatory system: dental anatomy and occlusion. Baltimore: Williams and Wilkins; 1969. p.94-115.

Appendix

1. The sphere fitting process based on least-squares theory

(1) Given a set of points $\{x_i, y_i, z_i\}_{i=1}^{m}, m \geqq 4$, not all the points are coplanar,

(2) Fit them with $(x-a)^2 + (y-b)^2 + (z-c)^2 = r^2$, where (a, b, c) is the sphere center and r is the sphere radius.

(3) The cost function to be minimized is

$$E(a, b, c, r) = \sum_{i=1}^{m} (L_i - r)^2$$

where $L_i = \sqrt{(x_i - a)^2 + (y_i - b)^2 + (z_i - c)^2}$.

(4) Take the partial derivative with respect to r to get

$$\frac{\partial E}{\partial r} = -2 \sum_{i=1}^{m} (L_i - r) \ ,$$

setting this to zero yields

$$r = \frac{1}{m} \sum_{i=1}^{m} L_i .$$

(5) Take the partial derivatives with respect to $a, b \ and \ c$ to obtain

$$\frac{\partial E}{\partial a} = -2 \sum_{i=1}^{m} (L_i - r) \frac{\partial L_i}{\partial a} = 2 \sum_{i=1}^{m} \left((x_i - a) + r \frac{\partial L_i}{\partial a} \right)$$

$$\frac{\partial E}{\partial b} = -2 \sum_{i=1}^{m} (L_i - r) \frac{\partial L_i}{\partial b} = 2 \sum_{i=1}^{m} \left((y_i - b) + r \frac{\partial L_i}{\partial b} \right)$$

$$\frac{\partial E}{\partial c} = -2\sum_{i=1}^{m}(L_i - r)\frac{\partial L_i}{\partial c} = 2\sum_{i=1}^{m}\left((z_i - c) + r\frac{\partial L_i}{\partial c}\right)$$

setting these to zeros yields

$$a = \frac{1}{m}\sum_{i=1}^{m} x_i + \frac{r}{m}\sum_{i=1}^{m}\frac{\partial L_i}{\partial a}$$

$$b = \frac{1}{m}\sum_{i=1}^{m} y_i + \frac{r}{m}\sum_{i=1}^{m}\frac{\partial L_i}{\partial b}$$

$$c = \tfrac{1}{m}\textstyle\sum_{i=1}^{m} z_i + \frac{r}{m}\sum_{i=1}^{m}\frac{\partial L_i}{\partial c}.$$

(6) Replacing r by $\frac{1}{m}\sum_{i=1}^{m} L_i$ and using $\frac{\partial L_i}{\partial a} = \frac{(a-x_i)}{L_i}$, $\frac{\partial L_i}{\partial b} = \frac{(b-y_i)}{L_i}$, and $\frac{\partial L_i}{\partial c} = \frac{(c-z_i)}{L_i}$, three nonlinear equations in a, b and c are obtained:

$$a = \bar{x} + \bar{L}\bar{L_a} \equiv F(a,b,c)$$

$$b = \bar{y} + \bar{L}\bar{L_b} \equiv G(a,b,c)$$

$$c = \bar{z} + \bar{L}\bar{L_c} \equiv H(a,b,c)$$

where

$$\bar{x} = \frac{1}{m}\sum_{i=1}^{m} x_i$$

$$\bar{y} = \frac{1}{m}\sum_{i=1}^{m} y_i$$

$$\bar{z} = \frac{1}{m}\sum_{i=1}^{m} z_i$$

$$\bar{L} = \frac{1}{m}\sum_{i=1}^{m} L_i$$

$$\bar{L_a} = \frac{1}{m}\sum_{i=1}^{m} \frac{(a - x_i)}{L_i}$$

$$\bar{L_b} = \frac{1}{m}\sum_{i=1}^{m} \frac{(b - y_i)}{L_i}$$

$$\bar{L_c} = \frac{1}{m}\sum_{i=1}^{m} \frac{(c - z_i)}{L_i}.$$

(7) Fixed point iteration is applied to solve these equations: $a_0 = \bar{x}$, $b_0 = \bar{y}$, $c_0 = \bar{z}$, and $a_{i+1} = F(a_i, b_i, c_i)$, $b_{i+1} = G(a_i, b_i, c_i)$, and $c_{i+1} = H(a_i, b_i, c_i)$ for $i \geq 0$. The iteration stops when the current center values and the updated values are almost the same. Note that the convergence and solution of this process are highly susceptible to the initial guess and the sample points. Although it was possible to introduce bias to the initial guess based on *a priori* knowledge that the sphere center should reside some distance above the virtual occlusal plane (VOP), in this study we chose to use the unbiased centroid as the initial guess, which was suitable for all data.

2. The planar fitting process based on the least-squares theory

By algebraic manipulation, it could be seen that the plane should pass through the centroid of the data points and its normal vector is the eigenvector corresponding to the smallest eigenvalue of the following covariance matrix M.

$$M$$

$$= \frac{1}{n}\begin{pmatrix} \sum_{i=1}^{n}(x_i - x_c)^2 & \sum_{i=1}^{n}(x_i - x_c)(y_i - y_c) & \sum_{i=1}^{n}(x_i - x_c)(z_i - z_c) \\ \sum_{i=1}^{n}(x_i - x_c)(y_i - y_c) & \sum_{i=1}^{n}(y_i - y_c)^2 & \sum_{i=1}^{n}(y_i - y_c)(z_i - z_c) \\ \sum_{i=1}^{n}(x_i - x_c)(z_i - z_c) & \sum_{i=1}^{n}(y_i - y_c)(z_i - z_c) & \sum_{i=1}^{n}(z_i - z_c)^2 \end{pmatrix}$$

where n is the number of data points, x_i, y_i, and z_i are the Cartesian coordinates of the data points, and x_c, y_c, z_c are the centroid coordinates.

Table 1 – Age distribution of the subjects.

	Mean ± SD	Min.	Max.
Males (n=41)	24.37 ± 0.73	23	26
Females (n=27)	24.26 ± 0.98	23	26
Total (n=68)	23.42 ± 0.84	23	26

SD, standard deviation ; Min., minimum age of the group ; Max., maximum age of the group ; n, the number of subjects.

Table 2 - Sex differences in the radii of occlusal curvatures.

	Monson's sphere**			Curve of Wilson in canines**			Curve of Wilson in molars**		
	Mean ± SD	5 % percentile	95 % percentile	Mean ± SD	5 % percentile	95 % percentile	Mean ± SD	5 % percentile	95 % percentile
Radius (mm)									
Males (n=41)	117.59 ± 27.23	73.80	166.27	114.03 ± 27.96	68.29	164.00	117.43 ± 27.27	73.48	166.24
Females (n=27)	100.70 ± 19.73	67.90	141.35	96.76 ± 20.50	61.83	138.39	100.56 ± 19.78	67.60	141.28
Total (n=68)	110.89 ± 25.75	72.04	164.63	107.18 ± 26.50	66.17	162.34	110.73 ± 25.79	71.74	164.53

Differences between males and females were examined using the Mann-Whitney U test (**$p < 0.01$).

Table 3 - Cuspal variation in the differences in the radius of occlusal curvature.

		Monson's sphere	Curve of Wilson in canines	Curve of Wilson in molars
Radius (mm)				
Cusp numbers of the second premolar	Two (n=45)	111.68 ± 24.28[a]	108.08 ± 24.96[c]	111.53 ± 24.32[e]
	Three (n=18)	106.36 ± 28.65[a]	102.28 ± 29.51[c]	106.19 ± 28.68[e]
	Two and three (n=5)	120.03 ± 30.49[a]	116.61 ± 31.32[c]	119.93 ± 30.53[e]
Cusp numbers of the second molar	Four (n=42)	110.84 ± 27.79[b]	107.12 ± 28.51[d]	110.69 ± 27.82[f]
	Five (n=23)	112.40 ± 23.64[b]	108.78 ± 24.52[d]	112.27 ± 23.69[f]
	Four and five (n=3)	99.81 ± 5.03[b]	95.66 ± 5.03[d]	99.63 ± 5.00[f]

Differences in cusp number were examined using the Kruskal-Wallis test. Same uppercase letters denote an insignificant difference within the same column ($p > 0.05$).

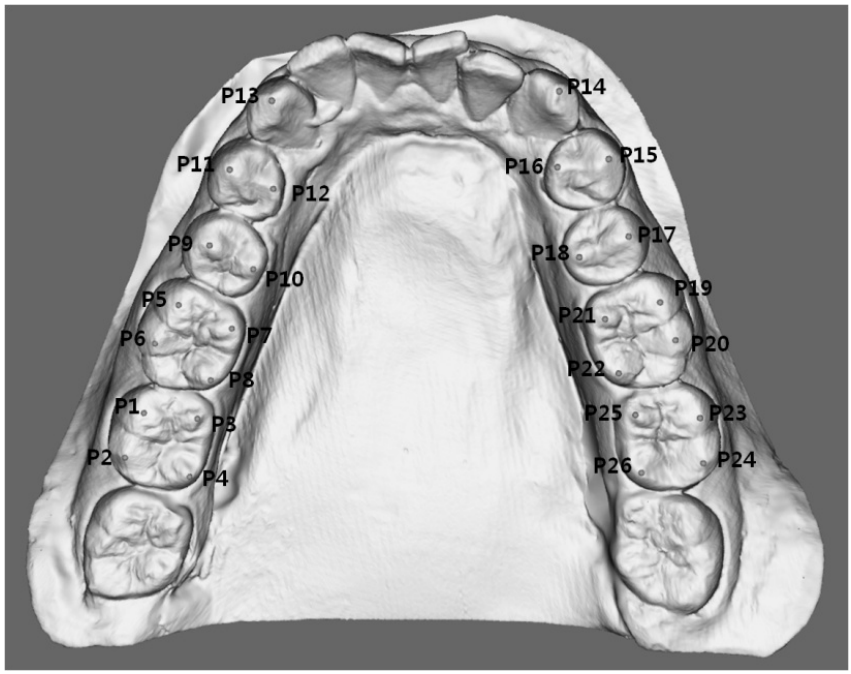

Fig. 1 - Virtual dental model and reference points. Cusp tips (P13 and P14) were identified on canines. Buccal cusp tips (P9, P11, P15 and P17) and lingual cusp tips (P10, P12, P16 and P18) were identified on premolars. Mesio-buccal cusp tips (P1, P5, P19 and P23), disto-buccal cusp tips (P2, P6, P20 and P24), mesio-lingual cusp tips (P3, P7, P21 and P25) and disto-lingual cusp tips (P4, P8, P22 and P26) were identified on molars.

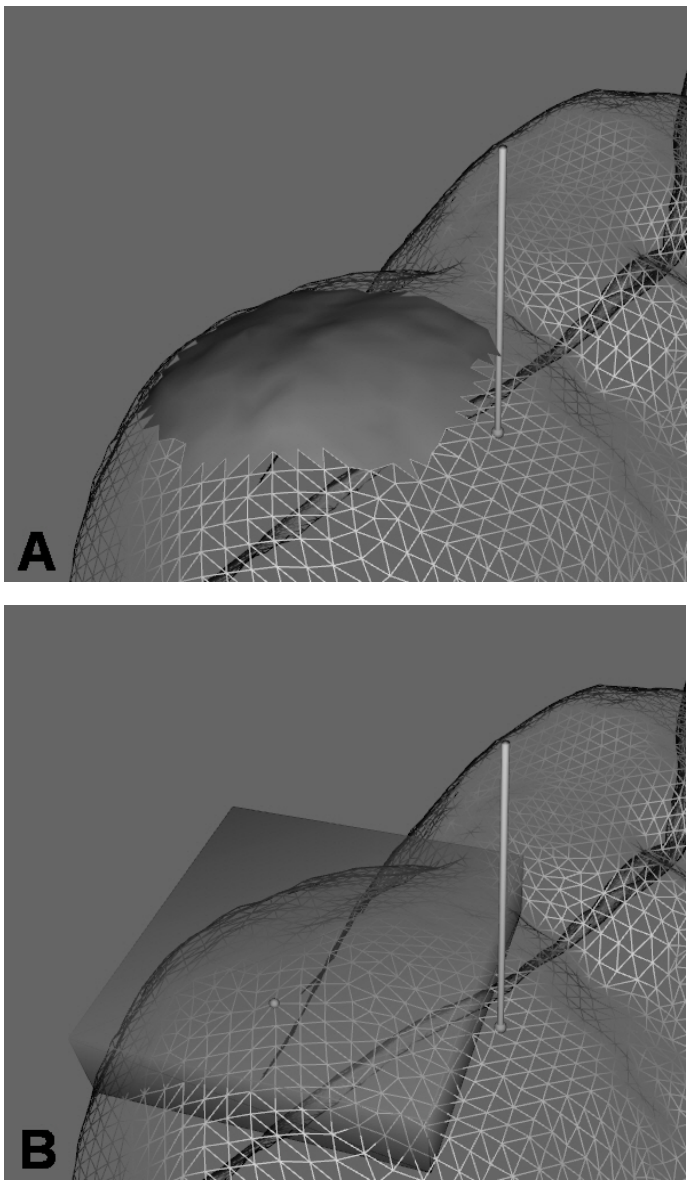

Fig. 2 - Reference point generation. (A) Operator-specified direction of vertex height and the region of interest from which the highest vertex was measured. (B) Cusp tip identified using the region of interest and measurement of vertex height with respect to the operator-defined direction.

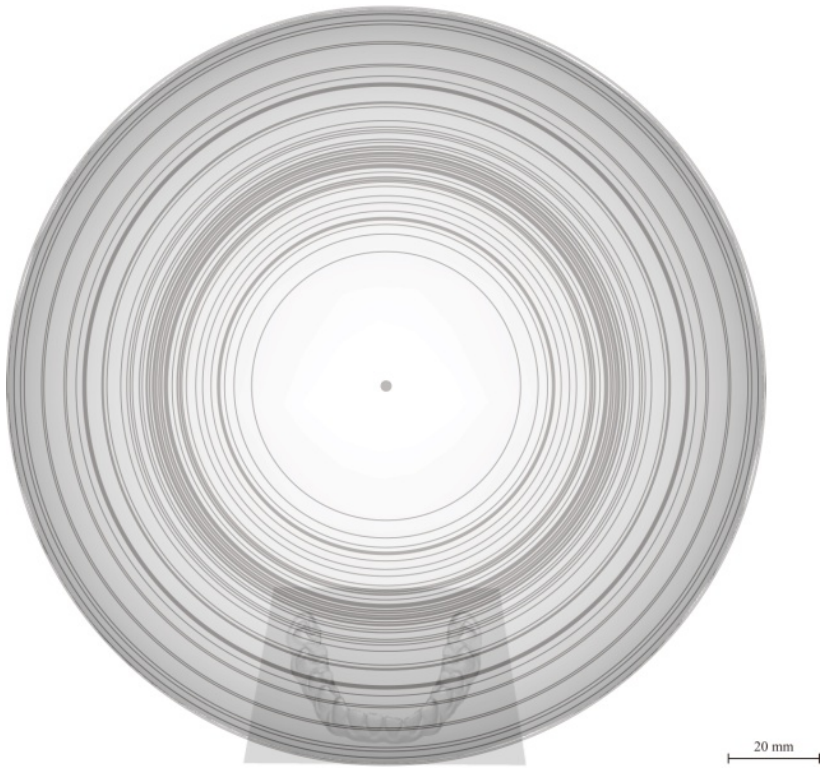

Fig. 3 - Various examples of fitted Monson’s sphere. The central points of 67 Monson’s sphere were superimposed on the largest sphere with respect to the central point to show the various radii of fitted spheres.

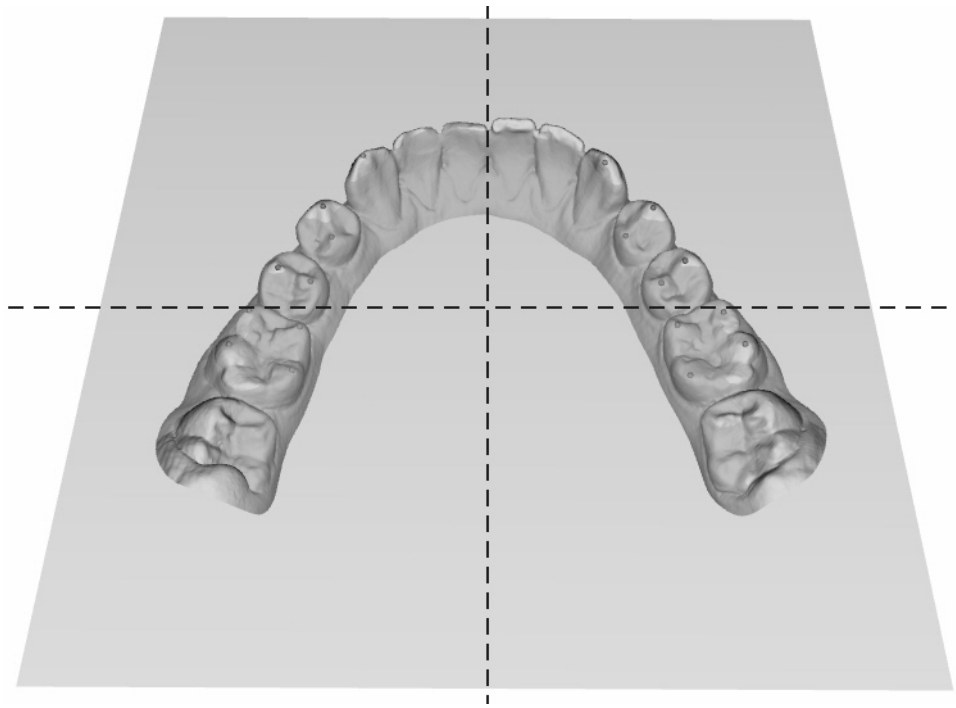

Fig. 4 - Virtual occlusal plane (VOP) computed by planar fitting of the cusp tips.

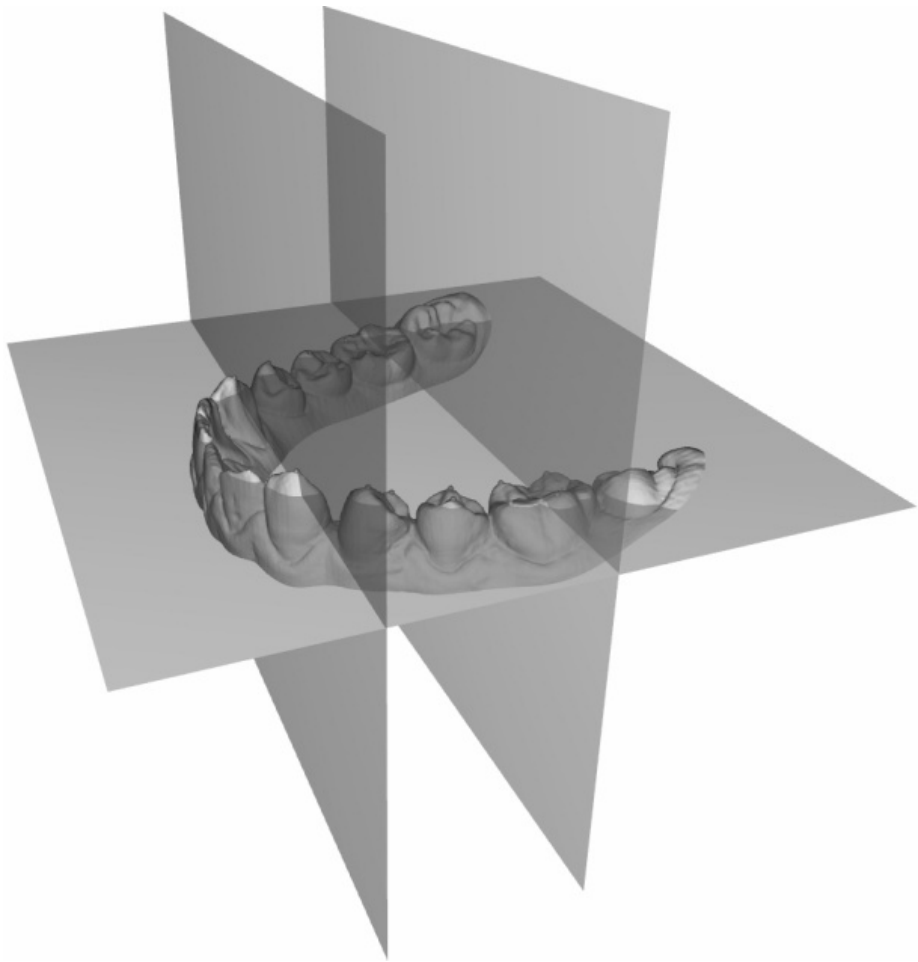

Fig. 5 - Virtual planes generated for the fitting of Wilson curves.

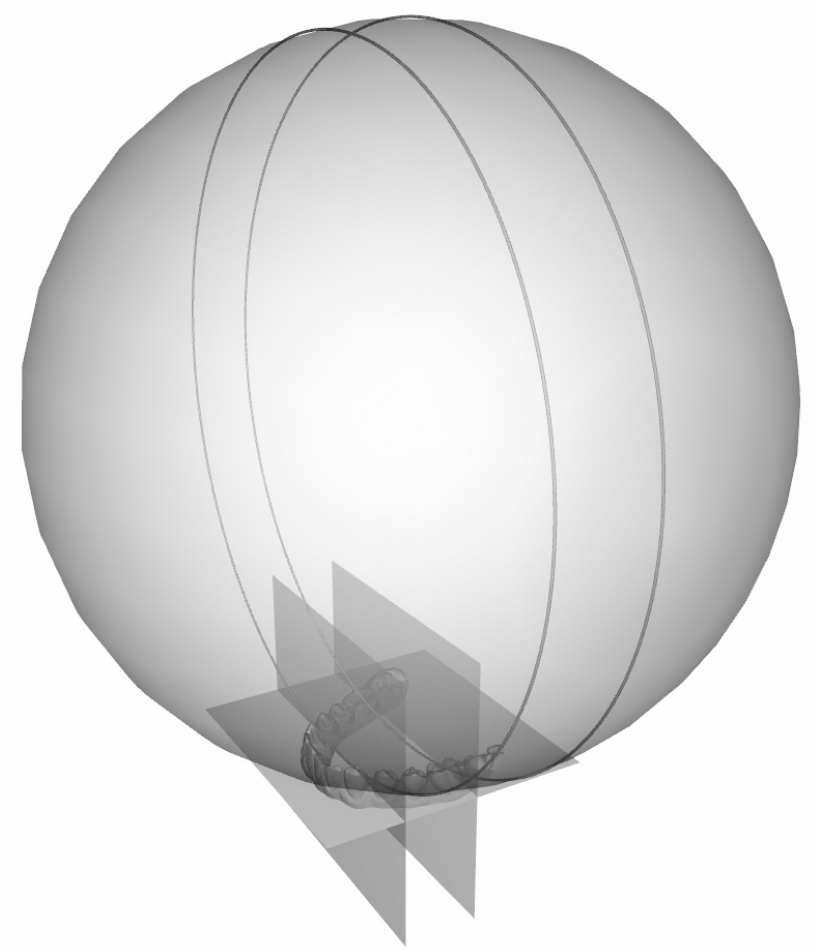

Fig. 6 - Wilson curves as intersection circles between Monson's sphere and relevant virtual plane

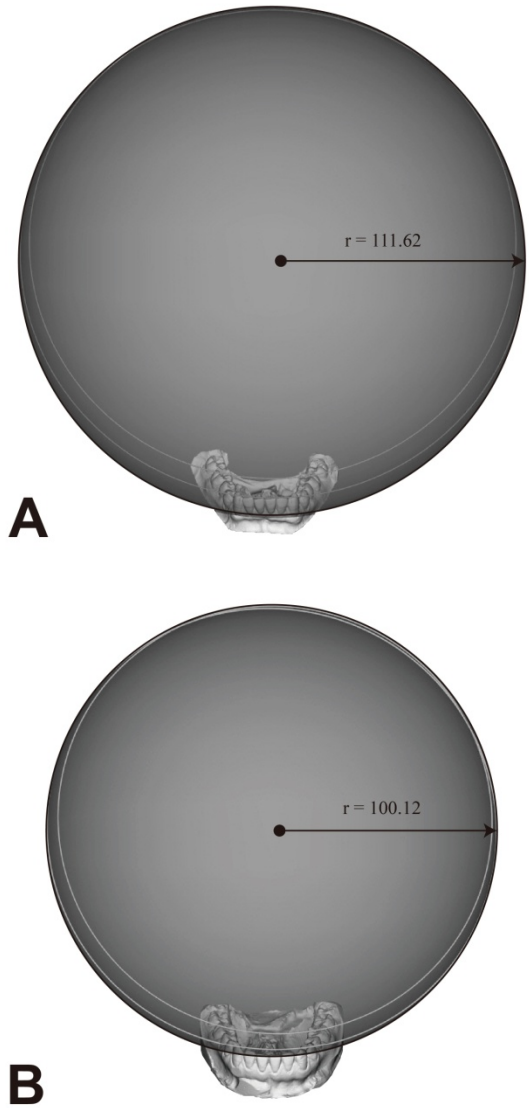

Fig. 7 - Sex differences in Monson's sphere, curve of Wilson in canines and curve of Wilson in molars. (A) Male sample. (B) Female sample. r : the radius of Monson’s sphere (mm).

국문초록

가상모형을 이용한 3차원적 몬슨 구에 대한 연구

남 신 은

서울대학교 대학원 치의학과 구강해부학 전공

지도교수 이 승 표

몬슨 구 (Monson's sphere)와 윌슨 만곡 (curve of Wilson)은 보철치료 시 구치부 교합의 재형성이나 의치 제작 시 시상 및 측방 조절만곡을 결정 할 때에 참고자료로 활용되고 있다. 본 연구는 가상모형과 자체 개발한 전용의 소프트웨어를 이용하여, 3차원적 몬슨 구와 윌슨 만곡을 재현하고 측정하고자 하였다. 만 23~26세 사이의 한국인 68명으로부터 얻은 하악 연구모형을 치과용 삼차원 재구성 시스템을 이용하여 가상모형으로 제작하였다. 자체 개발한 전용의 소프트웨어를 이용하여 가상모형상에 26개의 표지점을 인지한 후, 최소자승법 (least-squares method)에 입각하여 모든 표지점을 포함하는 근사 구 (fitted sphere)를 얻어 3차원적 몬슨 구를 재현하였다. 윌슨 만곡을 재현하기 위해 먼저 견치와 제1대구치 부위에서 가상교합평면에 직교하는 두 개의 가상수직평면을 생성한 후, 몬슨 구와 두 가상수직평면이 이루는 교차 원 (intersecting circle)을 얻어 두 개의 윌슨 만곡을 재현하였다. 몬슨 구와 윌슨 만곡의 크기에 남녀간의 유의한 차이가 있는지를 알아보기 위해 Mann-Whitney 검정을, 구치부 치아 내에서 교두의 개수에 따른 차이를 알아보기 위해 Kruskal-Wallis 검정을 시행하였다. 유의수준은 a = 0.05를

기준으로 통계적 유의성을 판정하였다. 한국인 남녀로부터 얻은 몬슨 구의 평균 반지름은 110.89 ± 25.75 mm (4.37 inch)였다. 모든 측정에서 반지름은 남녀 그룹 간에 유의한 차이를 보였으며 ($p<0.01$), 남자 그룹에서 최소 16.87 mm, 최대 17.27 mm가 더 크게 나타났다. 또한 하악 제2소구치와 제2대구치에서 보이는 교두 개수의 변이는 교합만곡에 유의한 영향을 주지 않았다 ($p>0.05$). 이번 연구를 통해 가상모형을 이용하여 3차원적 몬슨 구를 재현하고 측정하는 알고리즘을 개발 하였으며, 한국인의 몬슨 구 반지름은 몬슨 (Monson)이 보고한 전통적인 값 (4-inch)보다는 크다는 것을 알 수 있었다.

주요어: 몬슨 구, 윌슨 만곡, 가상모형, 알고리즘

학 번: 2007-23381